NANO LETTERS

2001
Vol. 1, No. 8
417−421

Preparation of the Xerogels of Nanocrystalline Titanias by the Removal of the Glycol at the Reaction Temperature after the Glycothermal Method and Their Enhanced Photocatalytic Activities

Shinji Iwamoto, Kazuko Saito, and Masashi Inoue*

Department of Energy and Hydrocarbon Chemistry, Graduate School of Engineering, Kyoto University, Yoshida, Kyoto 606-8501, Japan

Koji Kagawa

The Kansai Electric Power Company, Inc., 3-11-20 Nyakuoji, Amagasaki 661-0974, Japan

Received April 14, 2001; *Revised Manuscript Received June 25, 2001*

ABSTRACT

Xerogels consisting of nanocrystalline silica-modified titanias were obtained by the reaction of titanium tetraisopropoxide and tetraethyl orthosilicate in 1,4-butanediol at 300 °C for 2 h in an autoclave, followed by the removal of the organic phase from the autoclave at the reaction temperature. The coagulation of the ultrafine particles due to the surface tension of the liquid between the particles in the drying stage was prevented, which contributes to the superior thermal stability and photocatalytic activity of the products.

Preparation of tinania is the subject of importance because of various catalytic applications of this material; for example, as the supports for the selective catalytic reduction (SCR) of NO_x with ammonia[1] and the selective oxidation of hydrocarbons,[2] and also as photocatalysts for various reactions.[3] In recent years, photocatalytic water purification using titania-based semiconductor catalysts has collected great attention because of the high effectiveness of the catalysts against various organic pollutants such as chlorinated organic substrates,[4] dyes,[5] pesticides,[6] and endocrine disrupters.[7] Many studies have been carried out to understand the correlation between the catalytic properties and the photocatalytic activity of various titanias. In general, large surface area and high crystallinity are required for the highly active photocatalyst. The former feature contributes to efficient adsorption of the reactants, and the latter affects the surface property that strongly influences the recombination rate of the photoexcited electron (e^-) and positive hole (h^+). The sol−gel method is one of the preparation methods that affords titanias with extremely high surface areas.[8−10] However, the thus-obtained titanias contained some amounts of the amorphous phase and their surface area decreased drastically on calcination to improve the crystallinity.

One of the authors has studied the thermal reactions of metal alkoxides in organic media such as glycols (glycothermal reaction) and demonstrated that various novel and characteristic crystalline products were obtained directly by these reactions.[11−16] By applying these reactions for the preparation of titanias, microcrystalline anatases having large surface areas and excellent thermal stabilities were obtained,[17−19] and their superior photocatalytic activities were shown for various reactions.[20,21] Recently, we have found that the reactions of titanium tetraisopropoxide (TIP) and tetraethyl orthosilicate (TEOS) in 1,4-butanediol afforded nanocrystalline silica-modified titania with the anatase structure and that the thus-obtained silica-modified titanias showed quite high thermal stabilities.[22,23] In this paper, a novel method for the preparation of the xerogels of the silica-modified titania nanocrystals and their superior thermal stability and photocatalytic activity are described.

Titanium tetraisopropoxide (TIP; 25 g) and an appropriate amount of tetraethyl orthosilicate (TEOS, Si/Ti atomic ratio of 0−0.2) were added to 100 mL of 1,4-butanediol (1,4-

* E-mail address: inoue@scl.kyoto-u.ac.jp.

10.1021/nl010025b CCC: $20.00
Published on Web 07/20/2001

Table 1: Physical Properties of Titania Samples Calcined at Various Temperatures

	phase[a]			BET surface area (m^2/g)				crystallite size (nm)				pore volume (ml/g) $d < 50$ nm[b] total[c]		bulk density (g/cm^3)	
sample	800 °C	1000 °C	1100 °C	300 °C	600 °C	800 °C	1000 °C	as-syn	600 °C	800 °C	1000 °C	600 °C	600 °C	600 °C[c]	600 °C[d]
GT(0)	A	R + A	R	92	62	12	2	17	22	95	250	0.19	1.15	0.711	0.66
GT(0.1)	A	A	A + R	186	185	148	47	8.4	8.8	9.1	116	0.58	1.49	0.570	0.48
XG(0)	A	A + R	R + A	79	80	51	17	18	19	35	83	0.29	7.87	0.123	0.077
XG(0.02)	A	A		106	112	88	52	15	16	21	39				
XG(0.04)	A	A		101	107	93	73	14	14	17	23	0.48	5.59	0.171	0.14
XG(0.06)	A	A		154	168	133	74	11	12	13	24				
XG(0.1)	A	A	A	149	151	121	65	11	11	11	57	0.66	4.74	0.200	0.14
XG(0.2)	A	A		149	190	179	78	10	10	10	22				

[a] A, anatase; R, rutile. [b] Calculated from the N_2 adsorption method. [c] Calculated from the mercury porosimetry. [d] Measured.

BG), and this mixture was placed in a 300 mL autoclave equipped with two valves, one of which was used as a gas inlet and the other was connected to a Liebig condenser of stainless tubing. After the atmosphere inside the autoclave was replaced with nitrogen, the mixture was heated at a rate of 2.3 °C/min to 300 °C and kept at that temperature for 2 h. The collection of the products was carried in two ways. In the first method, after the assembly was cooled, the resulting powders were collected by centrifugation, washed with methanol or ammoniacal methanol and then air-dried. The thus-obtained products are designated as GT(x), where x is the Si/Ti charged ratio. In the second method, after the glycothermal reaction, the valve of the autoclave was slightly opened to remove the organic vapor from the autoclave by flash evaporation while keeping the autoclave temperature at 300 °C. When the pressure inside decreased to an atmospheric level, the autoclave was pressurized with nitrogen (~30 kg/cm^2) and nitrogen was released to ensure the removal of all the volatile matter. The assembly was cooled to the room temperature while the product was kept under slight pressure of nitrogen. The products were obtained directly as bulky solid and the thus-obtained products are designated as XG(x), where x is the Si/Ti charged ratio. The calcination of the products was carried out in a box furnace in air: the product was heated at a rate of 10 °C/min to a desired temperature and kept at that temperature for 30 min. The calcined samples are designated by adding "-(calcination temperature)" after the sample names; e.g., GT(0.1)-600 means the GT(0.1) sample calcined at 600 °C.

Powder X-ray diffraction (XRD) patterns were recorded on a Shimadzu XD-D1 diffractometer using CuKα radiation and a carbon-monochromator. The crystallite size was calculated by the Scherrer equation from the half-height width of the (101) diffraction peak of anatase after correction for the instrumental broadening. The specific surface area was calculated using the BET single-point method on the basis of the nitrogen uptake measured at 77 K using a Micromeritics Flowsorb II 2300. The pore-size distribution of the samples was calculated by the BJH method on the basis of the desorption branch of the N_2 adsorption isotherm obtained by a gas sorption system, Qantachrome Autosorb-1. The pore-size distribution was also determined by a mercury porosimeter, Micromeritics Autopore III 9240. Photocatalytic decomposition of acetic acid was carried out as follows. A suspension containing 0.3 mg of the catalyst in 5 mL of water was placed in a Pyrex test tube. To

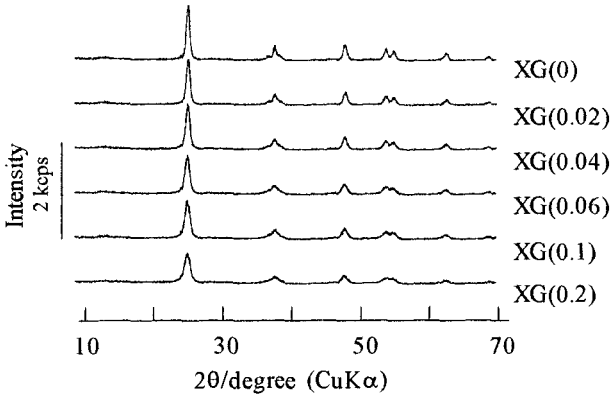

Figure 1. XRD patterns of the as-synthesized xerogel products obtained by the glycothermal reaction followed by removal of the organic solvent at the reaction temperature.

eliminate the organic moieties remaining on the surface of the catalyst, it was irradiated with a 500 W high-pressure mercury arc lamp at 25 °C under magnetic stirring. After confirming no further carbon dioxide formation from the catalyst, 15 mmol of acetic acid was added to the suspension and the test tube was closed with a rubber septum. The suspension was irradiated again at 25 °C, and the amounts of carbon dioxide in the gas phase in the test tube were monitored with a gas chromatograph (Shimadzu GC-8A with a Porapak Q column). JRC-TIO4 (equivalent to Degussa P-25) was taken as a reference to evaluate the photocatalytic activity of the catalysts prepared in this study.

As reported previously,[22] the silica-modified titanias prepared by the glycothermal method are nanocrystalline particles having the anatase structure, and therefore, the suspension of the as-synthesized products in methanol was relatively stable. After being air-dried, however, the suspension turned into a stiff solid. The coagulation of the fine particles took place during the drying stage due to the surface tension of the liquid between the particles.[24] On the other hand, the XG(x) products prepared by the glycothermal method followed by the removal of the organic phase from the autoclave were very bulky solid, brownish-grey in color, and easily turned into fine powders by hand.

In Figure 1, the XRD patterns of the as-synthesized XG(x), $x = 0$ to 0.2, are depicted, which show that all the products had the anatase structure. No indication of the presence of the other crystalline products or amorphous phase was observed, as was the case for the silica-modified titanias

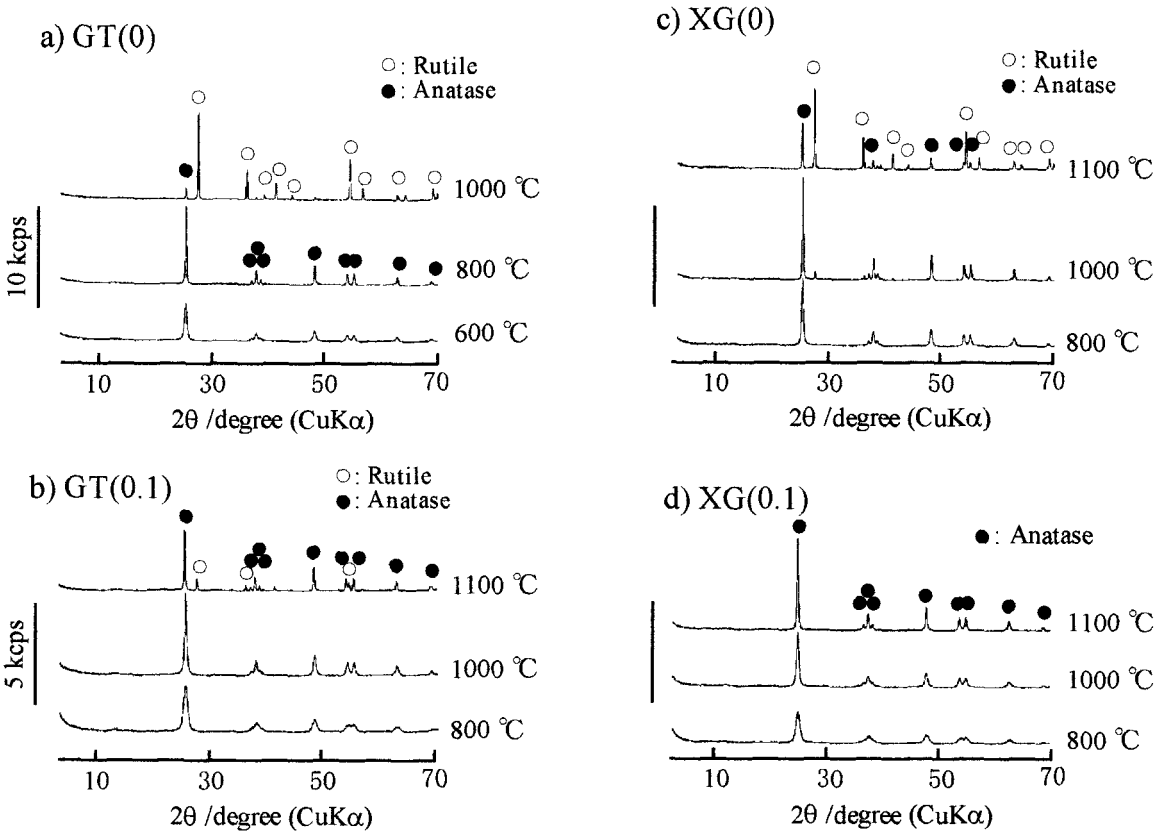

Figure 2. XRD patterns of the titania samples calcined at high temperatures.

prepared by the glycothermal method, GT(x).[22] The crystallite sizes of the XG(x), shown in Table 1, ranged from 10 to 18 nm, indicating that the products were nanocrystals. With increasing in the amount of the TEOS addition, the crystallite size decreased. This tendency was also observed for the glycothermal products, indicating that crystallization mechanism was not affected by the removal of the glycol at the reaction temperature. Slight increase in the crystallite size of the XG(x) as compared with the corresponding GT(x) sample can be attributed to the prolonged reaction time and the overheating at the final stage of the product recovery.

The XRD patterns and some physical properties of the products calcined at high temperatures are shown in Figure 2 and Table 1, respectively. The surface area of the GT(0) decreased from 91 to 12 m^2/g with partial transformation from anatase to rutile on calcination at 800 °C. After calcination at 1000 °C, the surface area further decreased and the transformation was mostly completed. On the other hand, the XG(0) preserved high surface areas of 51 and 17 m^2/g after calcination at 800 and 1000 °C, respectively, and the phase transformation was remarkably retarded as compared with the GT(0). Even after calcination at 1100 °C the transformation to rutile was not completed.

The enhanced thermal stability by the silica-modification has been demonstrated for the glycothermal products.[22] In the case of silica-modified XG(x) samples, further improvement of the thermal stability was observed. For example, the XG(0.1) preserved a quite large surface area of 65 m^2/g after calcination at 1000 °C, and this material preserved the anatase structure even after calcination at 1100 °C.

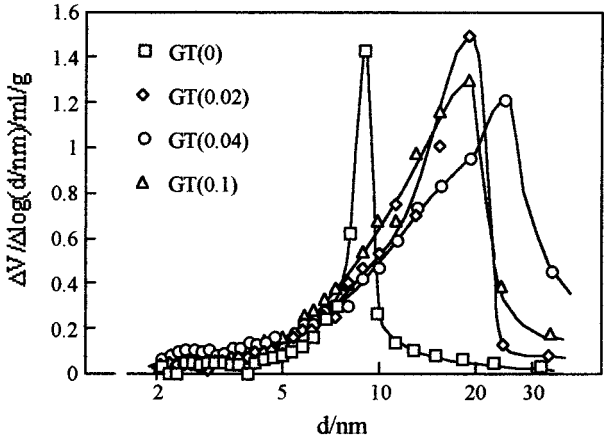

Figure 3. Pore size distributions of the GT(x)-600s calculated on the basis of desorption branch of the N_2 adsorption isotherm.

The pore-size distributions of the GT(x)-600, $x = 0$, 0.02, 0.04, 0.1, calculated from the N_2 adsorption isotherm, are shown in Figure 3. The GT(0)-600 has a sharp peak at the pore diameter of 9 nm. This value is a half of the crystallite size of this material (17 nm), and the pores in this range are attributed to the voids between tightly coagulated nanoparticles. In the case of the silica-modified GT(x), the pore-size distributed in a wide range and the mode pore diameter was observed around 20 nm. This size is twice as large as the size of the primary particles of these samples, and therefore, these mesopores seem to be formed in the space between loosely coagulated particles.

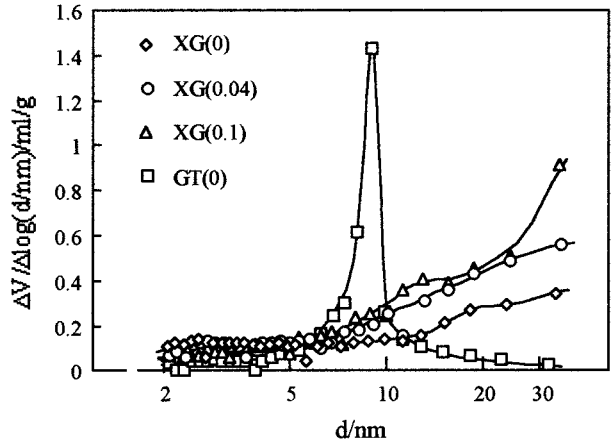

Figure 4. Pore size distributions of the XG(x)-600s calculated on the basis of desorption branch of the N_2 adsorption isotherm.

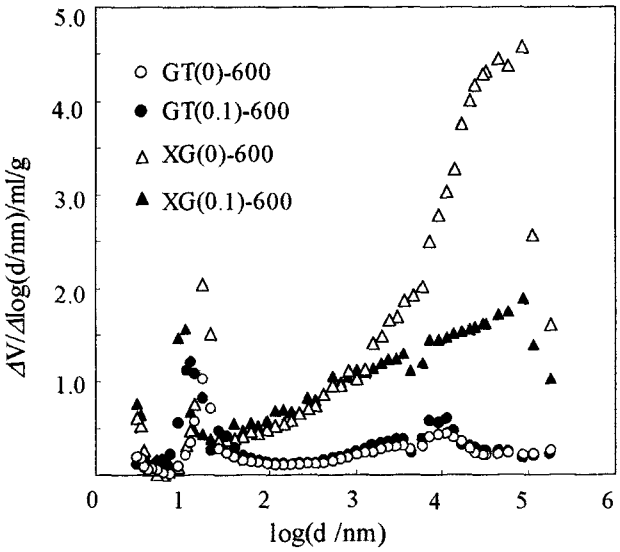

Figure 5. Pore size distributions of the XG(x)-600s determined by the mercury porosimetry.

Figure 4 shows the pore distribution of the XG(x)-600s calculated from the N_2 adsorption isotherm. No clear distribution peaks were observed in the mesopore range, indicating that coagulation during drying of wet gels due to the surface tension of the liquid[24] was effectively prevented. Figure 5 shows the pore-size distribution of the products measured by the mercury porosimetry. In the mesopore range, peaks are observed at 17, 12, 17, and 11 nm for GT(0), GT(0.1), XG(0), and XG(0.1), respectively. These sizes correspond quite well to the crystallite sizes of these samples, indicating that these peaks are not due to the pore structure but are attributed to the collapse of the coagulated structure into primary particles by applied high pressure of mercury. More noteworthy is that XG(0) and XG(0.1) exhibited significant volumes of pores in the macropore range, which also suggests that the primary particles were very loosely packed in XG(x) samples. The total pore volumes of XG(x), shown in Table 1, are much larger than those of GT(x) samples. Since the sintering starts at the contact points between particles, the low bulk density and the large pore

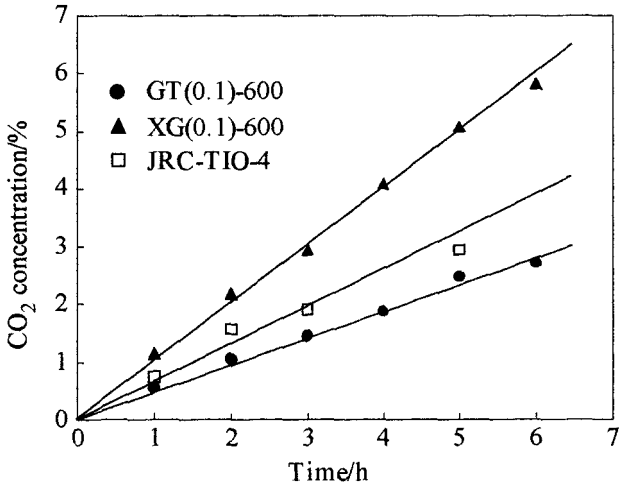

Figure 6. CO_2 formation via the photocatalytic oxidation of acetic acid in the aqueous suspension of GT(0.1) and XG(0.1).

size of the xerogel samples contribute to their superior thermal stabilities.

The time dependence of CO_2 formation via the photocatalytic decomposition of acetic acid in the suspension of GT(0.1) and XG(0.1) are compared in Figure 6. The amount of CO_2 linearly increased with the irradiation time for each catalyst. Kominami et al. also found that the reaction rate of the photocatalytic oxidation of acetic acid in titania suspension obeyed a pseudo-zero-order kinetics with the acetic acid concentration.[18,20] Apparently the XG(0.1) catalyst exhibited much higher activity than GT(0.1) and JRC-TIO4. Since GT(x) and XG(x) were prepared by essentially the same procedure but with different drying processes, both products should have the same chemical properties. Therefore, the difference in photocatalytic activities of these two samples should be attributed to the physical properties of the samples. When one assumes that the reaction of the adsorbed species with the photoexcited electron and/or hole is fast, the overall reaction rate will be limited by the diffusion of the reactant and/or the product (CO_2). Therefore, a higher rate is expected for XG(x) because of their quite large pore sizes.

When the stirring of the suspension was stopped, relatively rapid sedimentation took place for GT(0.1), while the suspension was relatively stable for XG(0.1). This result suggests high dispersibility of XG(0.1) in the suspension because of quite loose packing of the primary particles in xerogel, and this feature is the another reason for higher photocatalytic activity of XG(x).

In Table 2, the photocatalytic activities of GT(x) and XG(x) calcined at different temperatures are compared. The activity of GT(0) decreased with the increase in calcination temperature, which seems to be due to the drastic decrease in the surface area and the phase transformation. In contrast, the XG(x) catalysts exhibited higher photocatalytic activities, even after calcination at high temperatures. For the XG(x) catalysts with $x = 0.02$ and 0.04, the activity rather increased according to the calcination temperature. The role of silica as the adsorption sites for organic compounds was suggested by Anderson et al.,[25] and this may be a possible reason for the enhanced activities, since we observed that the proportion

Table 2: Relative Activities for Photocatalytic Oxidation of Acetic Acid[a]

	calcination temperature			
sample	as-syn	600 °C	800 °C	1000 °C
GT(0)	1.1	0.07		
GT(0.1)	0.8	0.9		
XG(0)	1.7	1.4	1.0	0.8
XG(0.02)	1.4	1.7	1.6	2.6
XG(0.04)	1.5	2.1	2.6	1.7
XG(0.06)	1.2	1.5	1.9	1.8
XG(0.1)	2.6	1.7	1.5	0.9
XG(0.2)	2.4	1.2	1.4	1.4

[a] Relative value to JRC-TIO-4.

of the silicon in the surface region increased with the increase in the calcination temperature. On the other hand, the activity of the catalysts with high silica contents decreased with the calcination temperature. The decreased activities in these cases are probably due to segregation that took place at high temperatures, yielding titania particles covered with smaller silica particles.

In conclusion, the xerogels consisting of nanocrystalline silica-modified titanias were obtained by the glycothermal reaction of TIP and TEOS in 1,4-BG at 300 °C followed by removal of the organic molecules by flash evaporation at the reaction temperature. The thus-obtained products exhibited extremely high thermal stability on calcination at high temperatures. This is because of the prevention of the coagulation, which takes place by the strong surface tension of the liquid between nanoparticles during drying of wet gels. A highly dispersed suspension was easily obtained from XG(*x*), and it showed improved photocatalytic activities.

References

(1) Bosch, H.; Janssen, F. *Catal. Today* **1988**, *2*, 369.
(2) Wachs, I. E.; Saleh, R. Y.; Chan, S. S.; Chersich, C. *Chemtech* **1985**, 756.
(3) Hoffmann, M. R.; Martin, S. T.; Choi, W.; Bahnemann, D. W. *Chem. Rev.* **1995**, *95*, 69.
(4) Guillard, C.; Disdier, J.; Herrmann, J.-M.; Lehaut, C.; Chopin, T.; Malato, S.; Blance, J. *Catal. Today* **1999**, *54*, 217.
(5) Qu, P.; Zhao, J.; Shen, T.; Hidaka, H. *J. Mol. Catal. A: Chem.* **1998**, *119*, 257.
(6) Tanaka, K.; Robledo, S. M.; Hisanaga, T.; Ali, R.; Ramli, Z.; Bakar, W. A. *J. Mol. Catal. A: Chem.* **1999**, *144*, 425.
(7) Coleman, H. M.; Eggins, B. R.; Bryne, J. A.; Palmer, F. L.; King, E. *Appl. Catal. B: Environmental* **2000**, *24*, L1.
(8) Zaharescu, M.; Crisan, M. *J. Sol-Gel Sci. Technol.* **1997**, *8*, 249.
(9) Dagan, G.; Tomkiewicz, M. *J. Non-Cryst. Solids* **1994**, *175*, 294.
(10) Montoya, I. A.; Viveros, T.; Domínguez, J. M.; Canales, L. A.; Schifter, I. *Catal. Lett.* **1992**, *15*, 207.
(11) Inoue, M.; Tanino, H.; Kondo, Y.; Inui, T. *J. Am. Ceram. Soc.* **1989**, *72*, 352.
(12) Inoue, M.; Kominami, H.; Inui, T. *J. Am. Ceram. Soc.* **1990**, *73*, 1100.
(13) Inoue, M.; Otsu, H.; Kominami, H.; Inui, T. *J. Mater. Sci. Lett.* **1992**, *11*, 269.
(14) Inoue, M.; Nakamura, T.; Otsu, H.; Kominami, H.; Inui, T. *Nippon Kagaku Kaishi* **1993**, 612.
(15) Inoue, M.; Otsu, H.; Kominami, H.; Inui, T. *J. Alloys Compd.* **1995**, *226*, 146.
(16) Inoue, M.; Nishikawa, T.; Nakamura, T.; Inui, T. *J. Am. Ceram. Soc.* **1997**, *80*, 2157.
(17) Inoue, M.; Komimami, H.; Otsu, H.; Inui, T. *Nippon Kagaku Kaishi* **1991**, 1364.
(18) Kominami, H.; Takada, Y.; Yamagiwa, H.; Kera, Y.; Inoue, M.; Inui, T. *J. Mater. Sci. Lett.* **1996**, *15*, 197.
(19) Kominami, H.; Kahno, M.; Takada, Y.; Inoue, M.; Inui, T.; Kera, Y. *Ind. Eng. Chem. Res.* **1999**, *38*, 3925.
(20) Kominami, H.; Kato, J.; Takada, Y.; Doushi, Y.; Ohtani, B.; Nishimoto, S.; Inoue, M.; Inui, T.; Kera, Y. *Catal. Lett.* **1997**, *46*, 235.
(21) Kominami, H.; Kato, J.; Murakami, S.; Kera, Y.; Inoue, M.; Inui, T.; Ohtani, B. *J. Mol. Catal. A: Chem.* **1999**, *144*, 162
(22) Iwamoto, S.; Tanakulrungsank, W.; Inoue, M.; Kagawa, K.; Praserthdam, P. *J. Mater. Sci. Lett.* **2000**, *19*, 1439.
(23) Iwamoto, Sh.; Iwamoto, Se.; Inoue, M.; Uemura, S.; Kagawa, K.; Tanakulrungsank, W.; Praserthdam, P. *Ceram. Trans.* **2000**, *115*, 643.
(24) Inoue, M.; Nakamura, T.; Inui, T. *Catal. Lett.* **2000**, *65*, 79.
(25) Anderson, C.; Bard, A. J. *J. Phys. Chem.* **1995**, *99*, 9882.

NL010025B